RNA (2000), *6*:563–570. Cambridge University Press. Printed in the USA.

Determination of preferential binding sites for anti-dsRNA antibodies on double-stranded RNA by scanning force microscopy

MICHAEL BONIN,[1] JÜRGEN OBERSTRAß,[1] NOEMI LUKACS,[3] KATJA EWERT,[2] EGBERT OESTERSCHULZE,[2] RAINER KASSING,[2] and WOLFGANG NELLEN[1]

[1]Department of Genetics, Kassel University, 34132 Kassel, Germany
[2]Department of Technical Physics, Kassel University, 34132 Kassel, Germany
[3]Institute for Plant Biology, Biological Research Center of the Hungarian Academy of Sciences, 6701 Szeged, Hungary

ABSTRACT

The monoclonal anti-dsRNA antibody J2 binds double-stranded RNAs (dsRNA) in an apparently sequence-nonspecific way. The mAb only recognizes antigens with double-stranded regions of at least 40 bp and its affinity to poly(A) poly(U) and to dsRNAs with mixed base pair composition is about tenfold higher than to poly(I) poly(C). Because no specific binding site could be determined, the number, the exact dimensions, and other distinct features of the binding sites on a given antigen are difficult to evaluate by biochemical methods. We therefore employed scanning force microscopy (SFM) as a method to analyze antibody–dsRNA interaction and protein–RNA binding in general. Several in vitro-synthesized dsRNA substrates, generated from the *Dictyostelium* PSV-A gene, were used. In addition to the expected sequence-nonspecific binding, imaging of the complexes indicated preferential binding of antibodies to the ends of dsRNA molecules as well as to certain internal sites. Analysis of 2,000 bound antibodies suggested that the consensus sequence of a preferential internal binding site is $A_2N_9A_3N_9A_2$, thus presenting A residues on one face of the helix. The site was verified by site-directed mutagenesis, which abolished preferential binding to this region. The data demonstrate that SFM can be efficiently used to identify and characterize binding sites for proteins with no or incomplete sequence specificity. This is especially the case for many proteins involved in RNA metabolism.

Keywords: AFM; anti-nucleic acid antibodies; RNA–protein interaction

INTRODUCTION

Elucidating the mechanism of antibody–RNA interaction is crucial to understanding the probable contribution of antibodies to pathological processes in some autoimmune diseases as well as for the general understanding of structural features that determine the specificity of RNA–protein recognition. Anti-nucleic acid antibodies play an important but still unclear role in the autoimmune disorder systemic lupus erythematosus (SLE; Gilbert et al., 1997). Understanding their interaction with DNA may provide better insight into the pathogenicity of the disease (Shlomchik et al., 1990; Chen et al., 1995; Zouali, 1997). In addition to sequence and structure analysis of anti-DNA antibodies, their binding mechanisms are of special interest (Ali et al., 1985; Stollar, 1986; Radic & Weigert, 1994). The major population of anti-nucleic acid antibodies is represented by DNA-specific species, but there are also antibodies directed against the left-handed helical Z-conformation (Z-DNA and Z-RNA) and against single-stranded (ss) or double-stranded (ds) RNA (Stollar, 1992). In contrast to DNA, which does not induce an immune response in healthy organisms, dsRNA is a relatively good antigen. dsRNA-specific antibodies like J2 recognize structural features common to most dsRNA species. Because many ssRNA- and dsRNA-binding proteins display apparently sequence-nonspecific interactions, anti-dsRNA antibodies may serve as a general model system to elucidate binding characteristics and binding mechanisms. This may improve their use in diagnosis and the general investigation of viral and metabolic dsRNAs (Schönborn et al., 1991; Lukacs, 1994).

RNA–protein interactions have become increasingly important as a result of the perception that gene regulation at the posttranscriptional level is significant. With the mechanisms of antisense RNA-mediated gene si-

Reprint requests to: Wolfgang Nellen, Department of Genetics, IBC, Kassel University, Heinrich-Plett-Str. 40, D-34125 Kassel, Germany; e-mail: nellen@hrz.uni-kassel.de.

lencing and the recent discovery of RNAi (Fire et al., 1998; Montgomery & Fire, 1998) as a specific inhibitor of gene expression, the role of dsRNA in cellular metabolism has become a central theme in research. The detection of dsRNA in cells or cellular extracts is difficult because artifacts may be generated during preparation and there are only indirect methods to demonstrate the presence of genuine dsRNA molecules. It has recently been shown that dsRNA-specific antibodies can be used to visualize dsRNA by in situ techniques (Lukacs, 1997). mAb J2, one of the antibodies used for in situ detection of dsRNA, has a binding preference for mixed-sequence dsRNA and poly(A)•poly(U) compared to poly(I)•poly(C) (Schönborn et al., 1991). A class of proteins showing a binding behavior similar to mAb J2 is characterized by one or more dsRNA-binding domains (dsRBD) (St Johnston et al., 1992; Finerty & Bass, 1997). These are domains of ~65–70 amino acids in an α-β-β-β-α configuration. High-resolution structural information is available for four of these proteins: RNAse III from *Escherichia coli* (Kharrat et al., 1995), the staufen protein from *Drosophila* (Bycroft et al., 1995), human dsRNA-dependent protein kinase (PKR; Nanduri et al., 1998), and Xlrbpa from *Xenopus* (Ryter & Schultz, 1998). For Xlrbpa co-crystallization with dsRNA showed that one domain covers 16 bp. For the other three proteins it is known that they not only recognize perfectly base paired dsRNA but also ssRNAs with defined secondary structures. It is, however, unclear how these proteins recognize different structures with similar specificity.

As a new method to investigate sequence-nonspecific dsRNA–protein interaction, we used scanning force microscopy (SFM) imaging. Previous SFM experiments on protein–nucleic acid interactions mostly concentrated on the recognition of DNA by RNA–polymerase (Guthold et al., 1994; Bustamante & Rivetti, 1996; Rippe et al., 1997) and on sequence-nonspecific DNA binding substances (Fritzsche et al., 1994; Allen et al., 1997; Hansma et al., 1998). This article presents the first in-depth investigation of a dsRNA-interacting protein using SFM and demonstrates an unexpected sequence preference that was not revealed as yet by biochemical methods.

RESULTS AND DISCUSSION

To confirm the specificity of mAb J2 for dsRNA under atomic force microscopy (AFM) conditions, we first investigated the affinity to DNA. In a 5-mM $MgCl_2$ solution, a considerable number of antibodies were found closely associated with DNA molecules (linearized plasmid containing the PSV-A gene) in AFM. With the addition of 100 mM Tris/Cl, pH 8, 150 mM NaCl, and 30 mM $MgCl_2$ to the binding reaction (corresponding to the salt concentrations used for antibody–dsRNA binding; see below), complex formation with DNA was completely abolished (data not shown). Antibody binding in low-salt solution was presumably due to charge interactions. This result suggested that the images reflect the binding in solution although they were taken in air.

We next analyzed the structure and integrity of the dsRNA molecules used in this study: three different in vitro-synthesized and hybridized transcripts of the PSV-A gene from *Dictyostelium* (Hildebrandt et al., 1991).

Values for the helix contour length measured on these dsRNAs (e.g., Fig. 2) are shown in Table 1. The calculated rise of 0.32, 0.29, and 0.30 nm/bp corresponded better to the A′ conformation (0.30 nm/bp) than to the standard A conformation (0.26 nm/bp). This was rather unexpected, as most authors propose from X-ray fiber data (Arnott et al., 1973) that dsRNA adopts the A conformation in solution. DNA molecules measured under the same conditions showed a contour length in agreement with the predicted B-helix conformation. One could thus assume that the values obtained for dsRNA also represent solution conditions and were not due to a conformational switch caused by drying of the sample. Since helix conformation is difficult to analyze by the standard solution structure determination methods (Tinoco et al., 1987), the discrepancy in the data may reflect differences in the techniques.

A standard method for the analysis of protein–nucleic acid interactions is the gel retardation or electrophoretic mobility shift assay (EMSA). An EMSA using mAb J2 and the dsRNA fragment EB-4-11 is shown in Figure 1. Although the dsRNA band disappeared upon incubation with the antibody, no bands of lower mobility, representing dsRNA–antibody complexes, were observed. RNA degradation during the incubation could be excluded, because single-stranded control RNAs remained intact. The most probable explanation for this observation is that the interaction between the bivalent antibody and the multivalent antigen resulted in a complex that was too large to migrate into the gel. Alternatively, the affinity of the antibodies was too low to maintain the complex, such that they dissociated during the gel run resulting in a homogenous, undetectable distribution over the entire lane. A third possibility was that the complexes were very heterogenous because of the number of mAbs bound to a single dsRNA and to the difference in migration depending on the

TABLE 1. Contour-length analysis of double-stranded nucleic acids.

	Number of base pairs	Mean of contour length	Rise per base pair
dsRNA EB4-11 (n = 168)	267	85 ± 3 nm	0.32 nm
dsRNA EB4-12 (n = 225)	389	114 ± 3 nm	0.29 nm
dsRNA EB4-1 (n = 260)	707	209 ± 6 nm	0.30 nm
dsDNA pGem3Z-EB4-11 (n = 61)	3,005	1026 ± 29 nm	0.34 nm

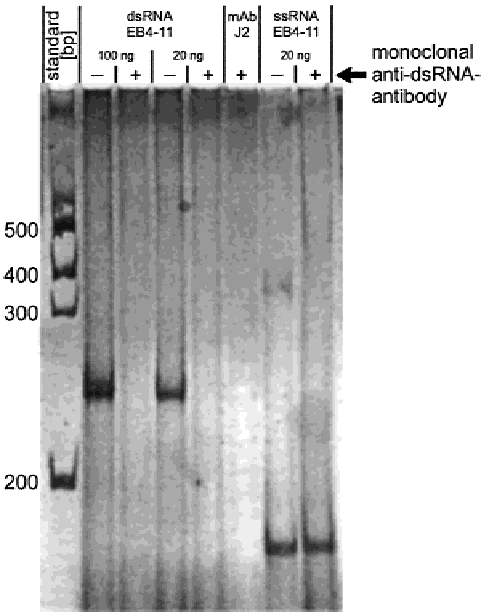

FIGURE 1. Gel retardation-assay. Native PAA gel-electrophoresis was performed with 20 ng and 100 ng of dsRNA EB4-11 incubated with and without 30 ng mAb J2. As a control 20 ng of single-stranded RNA (T7 transcript) were used. Lane J2 contains mAb only. The gel was stained with silver nitrate.

position where the antibody had bound. This would again result in a homogenous, undetectable smear over the entire lane. Antibodies directed against nucleic acids have been successfully used to generate distinct complex bands in EMSA on short DNA and DNA/RNA hybrids (Nordheim & Meese, 1988; Sanford et al., 1988). The disappearance of the antigen in our experiment only indirectly showed complex formation of dsRNA and mAb J2. This approach could, therefore, not answer questions about binding numbers, distribution of antibodies along the dsRNA molecule, and potential structural changes of the antigen upon binding.

We therefore used SFM imaging to investigate the J2-dsRNA interaction. In Figure 2, different dsRNA molecule species with various numbers of bound antibodies are shown. Figure 2a is an overview showing 267-bp dsRNA molecules most of which are occupied by at least one antibody. Figure 2b,c,d shows detailed views of the three different dsRNA species evaluated. In Figure 2b, a 707-bp molecule with two antibodies bound on opposite sides of the double strand is depicted; the location of binding corresponds to segments 7 and 8 (defined in Fig. 3a). Figure 2c shows the 389-bp dsRNA species with an internally bound mAb on two molecules; the position corresponds to segment 7 in Figure 3c. In Figure 2d, 267-bp molecules, all with mAbs bound to the ends, are seen. Figure 2e gives a three-dimensional impression as a surface plot of a 707-bp molecule with one antibody bound to an end and one to segment 3. Figure 2f shows high loading of six antibodies on a 627-bp dsRNA. The maximal binding number was difficult to determine because the high antibody concentrations required disturbed the image. Furthermore, it was no longer possible to unambiguously distinguish between bound molecules and antibodies that were fortuitously located close to the dsRNA molecule. Because binding reactions were done in solution, the entire surface of the helix was available for interaction with the protein. Theoretically, simultaneous binding on different sides of the RNA could interfere with attachment to the substrate or displace interacting antibodies. It was thus not feasible to unambiguously determine the closest possible binding of two antibodies to the RNA. We therefore measured the minimal contour length covered by the antibody; with 43 bp this also represents the maximal extent of the binding site. By electron microscopy, binding sites of 48 bp for IgG molecules and of 42.5 bp for two antigen determinants of an IgM were determined (Nahon-Merlin et al., 1980). In contrast to many other proteins binding to double-stranded nucleic acids (Steitz, 1993), the J2 antibody did not induce obvious bending or kinking of the dsRNA. Bending has been observed with an anti-Z-DNA antibody, the only other anti-nucleic acid antibody studied so far by SFM (Pietrasanta et al., 1994).

In Figure 2d, all antibodies are located at the end of the dsRNAs. End binding was also frequently observed in Figure 2a and is shown in Figure 2e,f. It was therefore tempting to assume a preferential binding of mAb J2 to the ends of dsRNA molecules. This property is also observed for other dsRNA binding proteins (Goodman et al., 1984; Michalowski et al., 1999) and could be explained by an increased flexibility at the ends, enabling changes in the pucker conformation (Nowakowski & Tinoco, 1997), by a difference in charge distribution due to the lack of a phosphate after end-trimming, or by other physico-chemical features that distinguish ends from internal sites.

The apparent binding preference to the ends and to a site 26 nm from an end (Fig. 2) prompted us to do a statistical evaluation of the distribution of binding sites. We scanned and evaluated several hundred dsRNAs according to the following procedure: Because the ends of the molecules could not be distinguished, “left” and “down” in the image were initially defined as the “left” end of the molecule. dsRNA molecules were then divided into consecutive segments of 13 nm (corresponding to 43 bp). The position of each bound antibody was determined and assigned to the corresponding segment. The distribution of bound mAbs is represented in Figure 3. As shown in the histogram in Figure 3a, there was indeed a strong preference for end binding. In addition, significantly increased binding was observed for segments 3 and 14 and segments 7–10. The symmetrical distribution of increased binding was expected, as the left and right ends of the molecules were randomly assigned. Using the subfragments of 267 and 389 bp, we attempted to further define the location of

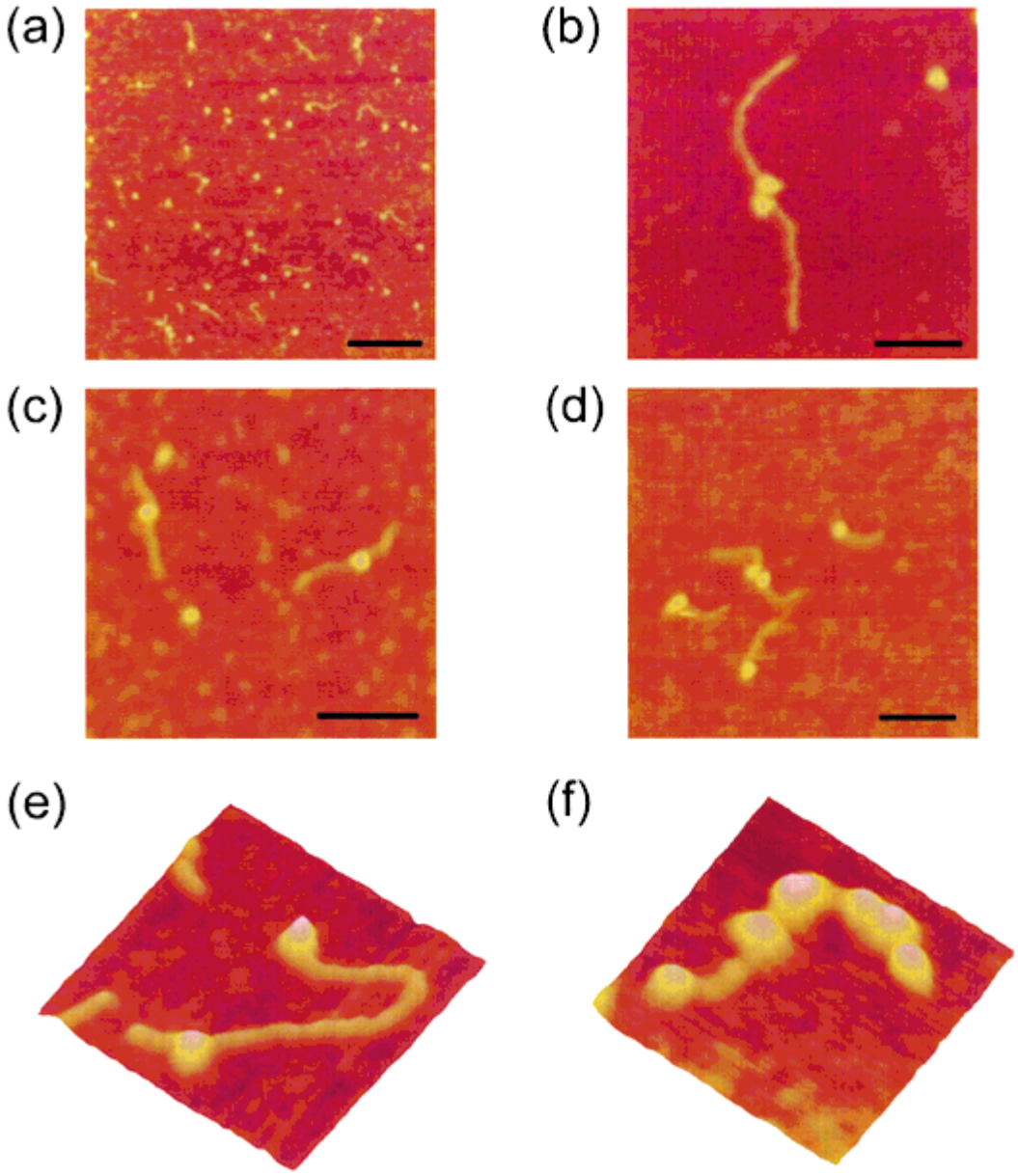

FIGURE 2. SFM images of dsRNA with bound mAb J2. **a**: Overview showing dsRNA EB4-11 molecules (267 bp) with bound antibodies. Scale bar is 200 nm. **b**: dsRNA EB4-1 (707 bp) with two mAbs bound to segments 7 and 8 (see Fig. 3a). Scale bar is 50 nm. **c**: dsRNA EB4-12 (389 bp) with internally bound mAb. Scale bar is 100 nm. **d**: dsRNA EB4-11 molecules with terminal mAb binding. Scale bar is 100 nm. **e**: Surface plot of an EB4-1 dsRNA molecule showing two mAbs bound to segment 3 and to the terminal position. Image size is 125 × 125 nm. **f**: Surface plot of 627-bp dsRNA molecule showing a high loading with six mAbs. Image size is 175 × 175 nm. The average height of the dsRNA and the antibody is 1.2 nm and 2 nm, respectively.

the preferential binding sites. dsRNA EB4-11 corresponded to one arm of dsRNA EB4-1, and dsRNA EB4-12 corresponded to the other. An internal fragment corresponding to almost two segments of dsRNA EB4-1 was not represented in the two subfragments. Measurements were done as described above, with the results given in Figure 3b,c. Again, a strong binding preference to the ends was observed. In addition, preferential binding was found in segments 3 and 4 of the dsRNA EB4-11 molecule, that is, 26 nm from either end. In contrast, the 389-bp dsRNA EB4-12 did not show increased internal binding. In comparison with the 707-bp molecule, this strongly suggested that segment 3 contained the strong internal binding site. We therefore postulated the orientation and binding site distribution presented in Figure 3d. For this graph, all antibodies bound 26 nm from one end were first assumed to have formed a complex with segment 3; subsequently the average sequence nonspecific binding calculated from all other nonpreferential binding sites

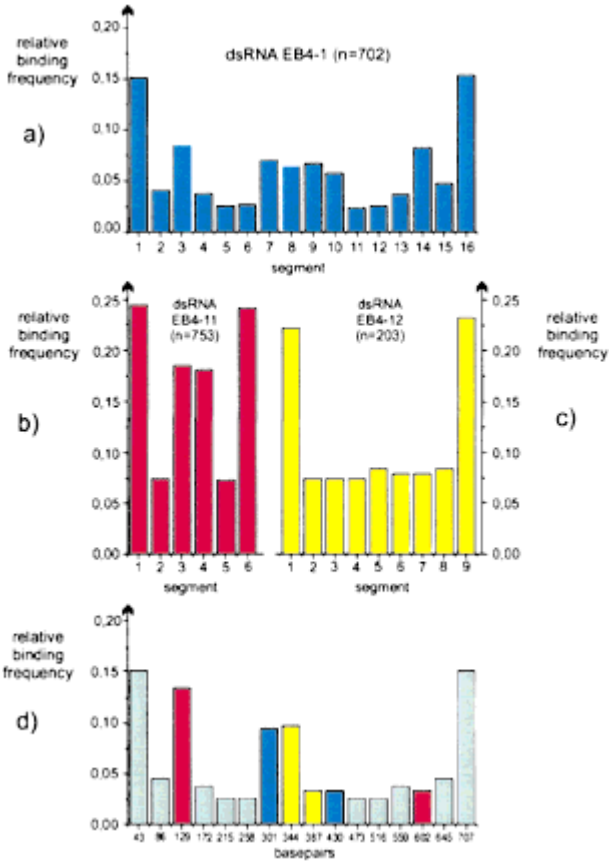

FIGURE 3. Analysis of antibody binding sites. **a**: Histogram of bound antibody distribution on the EB4-1 dsRNA molecule. Relative binding frequencies are given. Orientation of the molecules was arbitrary assigned as described in the text. N represent the total number of antibodies bound. A total of 408 dsRNA molecules were analyzed. **b**: Same analysis for the EB4-11 dsRNA (267 bp) molecule. A total of 1,267 dsRNA molecules were analyzed. This molecule contains the proximal 259 bp of the EB4-1 dsRNA molecule. **c**: Same analysis for the EB4-12 dsRNA (389 bp) molecule. A total number of 256 dsRNA molecules was analyzed. This molecule contains the distal 381 bp of the EB4-1 dsRNA. The apparent symmetry of the histogram is due to the arbitrary assignment of the ends. **d**: Model of binding site distribution derived from **a**, **b**, and **c** resulting in an oriented molecule. Antibodies counts for segments 3 and 14 were added, sequence-nonspecific binding was subtracted, and the relative binding frequency was assigned to segment 3 (corresponding to bp 87–129, red). The calculated sequence-nonspecific binding was assigned to segment 14 (red). The same procedure was applied to segments 7 and 10 (blue) and 8 and 9 (yellow). Sequence-nonspecific binding is the mean value of antibodies bound to segments other than ends and preferential binding sites.

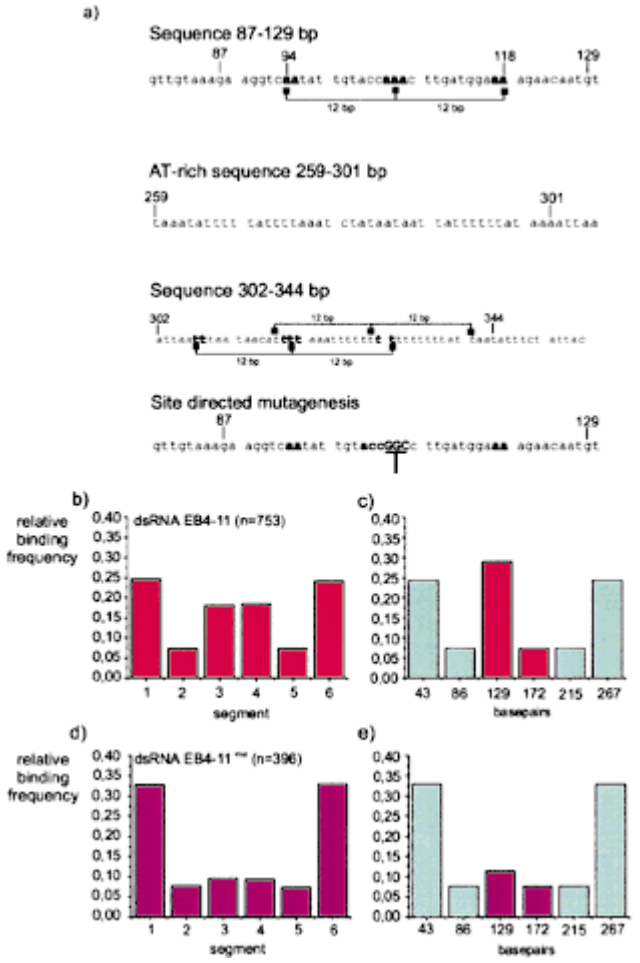

FIGURE 4. Determination of preferential binding and site-directed mutagenesis. **a**: Sequences of the putative preferential binding sites in segment 3 (positions 87–129), segment 7 (positions 259–301) and segment 8 (positions 302–344) are depicted. Brackets indicate the $A_2N_9A_3N_9A_2$ motif. The mutation introduced into the 87–129-bp putative binding site is shown in the bottom line. **b**: Arbitrary assignment of binding sites within dsRNA EB4-11 (267 bp) (as in Fig. 3b). **c**: Model of binding site distribution for EB4-11 dsRNA, similar to Fig. 3d. **d**: Arbitrary assignment of binding sites within EB4-11^{mut} after site-directed mutagenesis. **e**: Model of binding site distribution for EB4-11^{mut} dsRNA (as in Fig. 3d).

was subtracted and assigned to segment 14 (position 602). For reasons explained below, antibodies bound at a distance from 77 to 103 nm were assigned to segments 7 and 8 (positions 301 and 344 in Fig. 3d) and the corresponding symmetrical sites (segments 9 and 10, positions 387 and 430) show the calculated average sequence nonspecific binding. These adjusted data suggest an approximately threefold binding preference for segment 3 (position 129) and a more than twofold binding preference for segments 7 and 8 (positions 301 and 344) compared to random sequences.

To further elucidate the basis of preferential internal binding, we screened the sequence for potential binding motifs in these areas. Assuming that antibodies would recognize one side of the double helix, we especially looked for sequence motifs spaced at a distance of 12 bp. At positions 94–118 (corresponding to segment 3, Fig. 3d) we found the sequence depicted in Figure 4a with the special feature of $A_2\ N_9\ A_3\ N_9\ A_2$ with A residues arranged at 12-bp spacing. In an A′ conformation, this would present A residues on one side of the dsRNA. Two similar overlapping motifs (Fig. 4a) were found at positions 307–331 and 317–341 (corresponding to segment 8, Fig. 3d) in the sequence, but nowhere else in the fragment. Though segment 7 was highly A and U rich, we did not detect the motif defined

above. Burkhoff and Tullius (1987) had shown that A tracts cause bending in double-stranded DNA. This is, however, not the case in double-stranded RNA (Wang et al., 1991) and could therefore not be considered as a structural feature mediating preferential antibody binding.

To confirm the hypothesis that the motif in segment 3 presented a high affinity sequence for the antibody, we changed the central A triplet in the 267-bp fragment EB4-11 by site-directed mutagenesis to GGC, resulting in the altered motif A_2 N_9 GGC N_9 A_2 (Fig. 4a). Binding assays clearly showed that the number of bound antibodies was significantly reduced (Fig. 4b,d). Adjusted data are presented in Figure 4c,e and demonstrate that binding was reduced ~2.5-fold in comparison to the wild-type sequence. After subtracting sequence nonspecific binding (see also legend to Fig. 3), the binding preference was reduced almost sixfold or by 83%. Though a minor binding preference remained, the results clearly demonstrated that the exchange of 3 nt almost abolished the high affinity for this site and further confirmed our previous assumption of the orientation of the molecule. The fact that we could not define a motif determining preferential binding to segment 7 suggests that other sequence combinations also result in preferential binding or that our definition of the preferential binding motif was too strict.

It should be noted that the definition of the binding site also supported our previous assumption that the antibody binds to one side of the double strand. This was also found for Xlrbpa cocrystallized with dsRNA, where binding was observed to two successive minor grooves on one face of the helix (Kharrat et al., 1995).

Antibody decoration at the ends of molecules also posed the problem of defining orientation and to distinguish between a very strong binding sequence at one end or a general affinity to end structures. However, because many molecules had antibodies bound to both ends, it was rather likely that there was no high preferential binding on one side. In addition, high affinity to the ends was also observed when transcripts were generated which had different polylinker sequences at the termini (data not shown). We therefore assume that both ends have similar affinity resulting in an ~3.8-fold preference for end binding compared to internal random sequences. Possibly, open ends of double-helical RNAs present a structure with high affinity for the antibody. Such structural features are apparently also presented by internal dsRNA–ssRNA junctions, for example, in molecules with an internal single-stranded loop, where similar preferential binding was observed (data not shown). It will be interesting to see if closed ends as in foldback or hairpin loops will abolish end binding preference.

MAb J2 has been described as a nonsequence-specific dsRNA-binding antibody with some preference for A- and U-rich sequences (Schönborn et al., 1991). Our data confirm these findings but add a specific sequence motif, $A_2N_9A_3N_9A_2$, which displays strong preferential binding. However, as demonstrated by the undefined binding site in segment 7, this element is not the only one with higher than average affinity.

MATERIALS AND METHODS

In vitro transcription was done with plasmids pGEM-3Z-EB4-1, pGem3Z-EB4-11, pGem3Z-EB4-12, and pGem-3Z-EB4-1del (Hildebrandt et al., 1991; Hildebrandt & Nellen, 1992). The constructs were digested with *Bam*HI or *Acc*65I, transcribed with T7 and SP6 RNA polymerase (MBI Fermentas, St. Leon-Rot), respectively, according to Hecker et al. (1988). The following complementary ssRNAs resulted from these reactions: IVT EB4-1s (724 nt), IVT EB4-1as (750 nt), IVT EB4-11s (283 nt), IVT EB4-11as (310 nt), IVT EB4-12s (406 nt), IVT EB4-12as (432 nt), IVT EB4-1dels (663 nt), and IVT EB4-1delas (689 nt). Equimolar amounts of the complementary strands were mixed and hybridized in TNE (100 mM NaCl, 50 mM Tris-HCl, pH 8.0, and 10 mM EDTA) by heating at 95 °C for 10 min and slow cooling to room temperature. After trimming single-stranded overhangs with RNase A (30 min at 37 °C) and subsequent phenol extraction, the following completely base-paired dsRNA molecules were obtained: dsRNA EB4-1 (707 bp), dsRNA EB4-11 (267 bp), dsRNA EB4-12 (389 bp), and dsRNA EB4-1del (627 bp). RNA was ethanol precipitated and redissolved in double-distilled water.

Samples for gel-retardation assays were prepared by incubation of 10^{-8} M (30 ng) mAb J2 (Schönborn et al., 1991) with 20 ng and 100 ng dsRNA in 1× PBS for 10 min. In a control reaction, 20 ng of ssRNA were used. Complexes were separated on a nondenaturing 6% PAGE at room temperature in 1× TBE (Theissen et al., 1989) for 2 h at 12 V/cm. The respective RNAs were also submitted to electrophoresis without mAb J2. Molecules were detected by silver staining (Hecker et al., 1988).

Site-directed mutagenesis of the preferential binding site was done according to the Stratagene Manual for the QuikChange kit (Stratagene GmbH, Heidelberg). To create restriction enzyme recognition sites within the J2 binding site of fragment EB4-11, the following oligonucleotides were designed: J2 Fw (31 nt), GGTCAATATTGTACC**GGC**CTTGATG GAAAAG, and J2 Rev (31 nt), CTTTTCCATCAAG**GCC**GGT ACAATATTGACC, and used for PCR reactions. The introduction of the mutation was verified by sequencing and the resulting construct was designated pGem3Z-EB4-11^{mut}.

dsRNA-antibody complexes were formed by combining 1.0–2.5 nM dsRNA and 35 nM mAb J2 in 1× TBS, 30 mM $MgCl_2$ at pH 8.0 for 10 min at room temperature. A 10-μL drop of the sample was placed for 1 min on a freshly cleaved, glow discharged (1 min, 0.3 mbar air) mica surface, washed with 1 mL MilliQ water and blown dry with nitrogen. Samples were scanned with a Nanoscope III multimode SFM (Digital Instruments, Santa Barbara, California) operated in the tapping mode using a J scanner with a 125 × 125 (x,y) × 5 (z) μm scan range or an E scanner with a 10 × 10 (x,y) × 2.5 (z) μm scan range. Microfabricated silicon tips with a force constant of ~42 N m^{-1} and a resonance frequency of ~320 kHz (Pointprobes; Nanosensors GmbH, Wetzlar) were used. The

free amplitude was ~100 nm, the setpoint was 30% below the free amplitude. Images (512 × 512 pixels) were taken at 1–2 Hz scanning frequency in the topographic mode in air (relative humidity 20–50%), and at room temperature (18–27 °C).

Images were processed with the Nanoscope software including the operations of plane fitting and flattening. Contour length measurement was done by drawing a traverse line along the skeleton of the molecule on the screen.

For quantitative analysis of antibody binding to the RNA, imaged molecules were subdivided into segments of 13 nm. Left and down was arbitrarily defined as segment 1. The number of antibodies found in each segment was counted and divided by the total number of bound antibodies (relative binding frequency).

ACKNOWLEDGMENTS

We thank A. Schaper and T. Jovin for their help and advice in setting up SFM for biological samples. This work was in part supported by a grant from the Deutsche Forschungsgemeinschaft (Ne285/4) to W.N. and by an Otto-Braun stipend to M.B.

Received October 27, 1999; returned for revision January 8, 2000; revised manuscript received January 24, 2000

REFERENCES

Ali R, Dersimonian H, Stollar BD. 1985. Binding of monoclonal antinative DNA autoantibodies to DNA of varying size and conformation. *Mol Immunol 22*:1415–1422.

Allen MJ, Bradbury EM, Balhorn R. 1997. AFM analysis of DNA-protamine complexes bound to mica. *Nucleic Acids Res 25*:2221–2226.

Arnott S, Hukins DWL, Dover SD, Fuller WRHA. 1973. Structures of synthetic polynucleotides in the A-RNA and A′-RNA conformations: X-ray diffraction analyses of the molecular conformations of polyadenylic acid • polyuridylic acid and polyinosinic acid • polycytidilic acid. *J Mol Biol 81*:107–122.

Burkhoff AM, Tullius TD. 1987. The unusual conformation adopted by the adenine tracts in kinetoplast DNA. *Cell 48*:935–943.

Bustamante C, Rivetti C. 1996. Visualizing protein–nucleic acid interactions on a large scale with the scanning force microscope. *Annu Rev Biophys Biomol Struct 25*:395–429.

Bycroft M, Grunert S, Murzin AG, Proctor M, St Johnston D. 1995. NMR solution structure of a dsRNA binding domain from *Drosophila staufen* protein reveals homology to the N-terminal domain of ribosomal protein S5 [published erratum appears in *EMBO J* 1995 *14*:4385]. *EMBO J 14*:3563–3571.

Chen C, Nagy Z, Radic MZ, Hardy RR, Huszar D, Camper SA, Weigert M. 1995. The site and stage of anti-DNA B-cell deletion. *Nucleic Acids Symp Ser 33*:106–108.

Finerty PJ Jr, Bass BL. 1997. A *Xenopus* zinc finger protein that specifically binds dsRNA and RNA–DNA hybrids. *J Mol Biol 271*:195–208.

Fire A, Xu S, Montgomery MK, Kostas SA, Driver SE, Mello CC. 1998. Potent and specific genetic interference by double-stranded RNA in *Caenorhabditis elegans* [see comments]. *Nature 391*:806–811.

Fritzsche W, Schaper A, Jovin TM. 1994. Probing chromatin with the scanning force microscope. *Chromosoma 103*:231–236.

Gilbert D, Brard F, Courville P, Joly P, Lauret P, Tron F. 1997. Do certain autoantibodies produced in the course of human autoimmune blistering skin diseases behave as adhesion molecules? *Ann NY Acad Sci 815*:506–508.

Goodman TC, Nagel L, Rappold W, Klotz G, Riesner D. 1984. Viroid replication. Equilibrium association constant and comparative activity measurements for the viroid-polymerase interaction. *Nucleic Acids Res 12*:6231–6246.

Guthold M, Bezanilla M, Erie DA, Jenkins B, Hansma HG, Bustamante C. 1994. Following the assembly of RNA polymerase–DNA complexes in aqueous solutions with the scanning force microscope. *Proc Natl Acad Sci USA 91*:12927–12931.

Hansma HG, Golan R, Hsieh W, Lollo CP, Mullen Ley P, Kwoh D. 1998. DNA condensation for gene therapy as monitored by atomic force microscopy. *Nucleic Acids Res 26*:2481–2487.

Hecker R, Wang ZM, Steger G, Riesner D. 1988. Analysis of RNA structures by temperature-gradient gel electrophoresis: Viroid replication and processing. *Gene 72*:59–74.

Hildebrandt M, Humbel BM, Nellen W. 1991. The *Dictyostelium discoideum* EB4 gene product and a truncated mutant form of the protein are localized in prespore vesicles but absent from mature spores. *Dev Biol 144*:212–214.

Hildebrandt M, Nellen W. 1992. Differential antisense transcription from the Dictyostelium EB4 gene locus: Implications on antisense-mediated regulation of mRNA stability. *Cell 69*:197–204.

Kharrat A, Macias MJ, Gibson TJ, Nilges M, Pastore A. 1995. Structure of the dsRNA binding domain of *E. coli* RNase III. *EMBO J 14*:3572–3584.

Lukacs N. 1994. Detection of virus infection in plants and differentiation between coexisting viruses by monoclonal antibodies to double-stranded RNA. *J Virol Methods 47*:255–272.

Lukacs N. 1997. Detection of sense:antisense duplexes by structure-specific anti-RNA antibodies. In: Lichtenstein C, Nellen W, eds. *Antisense technology: A practical approach*. New York: Oxford University Press. pp 281–294.

Michalowski S, Miller JW, Urbinati CR, Paliouras M, Swanson MS, Griffith J. 1999. Visualization of double-stranded RNAs from the myotonic dystrophy protein kinase gene and interactions with CUG-binding protein. *Nucleic Acids Res 27*:3534–3542.

Montgomery MK, Fire A. 1998. Double-stranded RNA as a mediator in sequence-specific genetic silencing and co-suppression. *Trends Genet 14*:255–258.

Nahon-Merlin E, Delain E, Coulaud D, Lacour F. 1980. Electron microscopy of the reactions of anti-poly A • poly U and poly I • poly C antibodies with synthetic polynucleotide complexes and natural acids. *Nucleic Acids Res 8*:1805–1822.

Nanduri S, Carpick BW, Yang Y, Williams BR, Qin J. 1998. Structure of the double-stranded RNA-binding domain of the protein kinase PKR reveals the molecular basis of its dsRNA-mediated activation. *EMBO J 17*:5458–5465.

Nordheim A, Meese K. 1988. Topoisomer gel retardation: Detection of anti-Z-DNA antibodies bound to Z-DNA within supercoiled DNA minicircles. *Nucleic Acids Res 16*:21–37.

Nowakowski J, Tinoco IJ. 1997. RNA structure and stability. *Semin Virol 8*:153–165.

Pietrasanta LI, Schaper A, Jovin TM. 1994. Probing specific molecular conformations with the scanning force microscope. Complexes of plasmid DNA and anti-Z-DNA antibodies. *Nucleic Acids Res 22*:3288–3292.

Radic MZ, Weigert M. 1994. Genetic and structural evidence for antigen selection of anti-DNA antibodies. *Annu Rev Immunol 12*:487–520.

Rippe K, Guthold M, von Hippel PH, Bustamante C. 1997. Transcriptional activation via DNA-looping: Visualization of intermediates in the activation pathway of *E. coli* RNA polymerase × sigma 54 holoenzyme by scanning force microscopy. *J Mol Biol 270*:125–138.

Ryter JM, Schultz SC. 1998. Molecular basis of double-stranded RNA–protein interactions: Structure of a dsRNA-binding domain complexed with dsRNA. *EMBO J 17*:7505–7513.

Sanford DG, Kotkow KJ, Stollar BD. 1988. Immunochemical detection of multiple conformations within a 36 base pair oligonucleotide. *Nucleic Acids Res 16*:10643–10655.

Schönborn J, Oberstraß J, Breyel E, Tittgen J, Schumacher J, Lukács N. 1991. Monoclonal antibodies to double-stranded RNA as probes of RNA structure in crude nucleic acid extracts. *Nucleic Acids Res 19*:2993–3000.

Shlomchik M, Mascelli M, Shan H, Radic MZ, Pisetsky D, Marshak Rothstein A, Weigert M. 1990. Anti-DNA antibodies from autoimmune mice arise by clonal expansion and somatic mutation. *J Exp Med 171*:265–292.

St Johnston D, Brown NH, Gall JG, Jantsch M. 1992. A conserved double-stranded RNA-binding domain. *Proc Natl Acad Sci USA 89*:10979–10983.

Steitz TA. 1993. Similarities and differences between RNA and DNA recognition by proteins. In: Gesteland RF, Atkins JF, eds. *The RNA world*. Cold Spring Harbor, New York: Cold Spring Harbor Laboratory Press. pp 219–238.

Stollar BD. 1986. Antibodies to DNA. *CRC Crit Rev Biochem 20*: 1–36.

Stollar BD. 1992. Immunochemical analyses of nucleic acids. *Prog Nucleic Acid Res Mol Biol 42*:39–77.

Theissen G, Richter A, Lukacs N. 1989. Degree of biotinylation in nucleic acids estimated by a gel retardation assay. *Anal Biochem 179*:98–105.

Tinoco I Jr, Davis PW, Hardin CC, Puglisi JD, Walker GT, Wyatt J. 1987. RNA structure from A to Z. *Cold Spring Harb Symp Quant Biol 52*:135–146.

Wang YH, Howard MT, Griffith JD. 1991. Phased adenine tracts in double-stranded RNA do not induce sequence-directed bending. *Biochemistry 30*:5443–5449.

Zouali M. 1997. The structure of human lupus anti-DNA antibodies. *Methods 11*:27–35.